Clinical assessment of lesion detectability in dynamic whole-body PET imaging using compartmental and Patlak parametric mapping

Neda Zaker, Fotis Kotasidis, Valentina Garibotto and Habib Zaidi†, *IEEE Fellow*

***Abstract*– Continuous Bed Motion (CBM) acquisition mode enables the simultaneous estimation of compartmental and graphical analysis kinetic parameters in whole-body (WB) dynamic PET imaging. Lesion detectability is one of the important characteristics when developing novel image acquisition protocols. In this work, we used clinical dynamic WB ^{18}F-FDG PET/CT studies to compare lesion detectability between Patlak graphical analysis and full compartmental modeling derived using a previously proposed methodology for hybrid macro- and micro-parametric imaging. The performance of these approaches in the context of lesion detection and false positive identification was compared to conventional static standardized uptake value (SUV) imaging. This study was conducted on 8 clinical whole-body ^{18}F-FDG PET/CT studies injected with 3.5 MBq/kg of ^{18}F-FDG. The total scan time including dynamic WB imaging lasted 80 minutes. An in-house developed MATLAB code was utilized to derive the micro- and macro-parametric maps. In total, 104 lesions were detected, among which 47 located in the bed position where all quantitative parameters were calculated, thus enabling comparative analysis. The evaluation encompassed visual interpretation performed by expert physicians as well as quantitative and statistical analysis. High correlation coefficients were observed between SUV_{max} and K_{imax} derived from generalized linear least square (GLLS) approach as well as K_i generated by Patlak graphical analysis. Moreover, three biopsy-proven malignant lesions located in the liver were not visible on static SUV images and Patlak maps while they were depicted on K_1 and k_2 maps. Our results demonstrate that full compartmental modeling has the potential to provide complementary information and in some cases more accurate diagnosis than conventional static SUV imaging and even Patlak graphical analysis.**

I. Introduction

Acquisition of tracer time activity curves (TACs), which is feasible using dynamic PET imaging, enables the estimation of macro- and micro-parametric parameters [1]. In clinical practice, static PET imaging, using semi-quantitative indices, such as standardized uptake value (SUV) is predominently used in clinial routine. Unfortunately, these indices don't capture the time varying tracer kinetics implicitly provided by PET imaging to better charecterize biological tissues. Recently, an updated protocol to dynamic WB imaging has been proposed [2]. This protocol involves an initial single-bed blood pool scan targeting both the pathology and blood pool (aorta or ventricles), followed by a series of temporally non-continuous WB passes at ever increasing time intervals. By this technique, the input function is obtained from the initial blood pool scan and the following CBM passes. Depending on the location of the pathology, the initial blood pool scan can be chosen in the heart region, ascending or descending aorta.WB Patlak parametric maps as well as micro-parameters for the initial single bed FOV covering the pathology can also be derived. Since, full compartmental modelling requires both full time course of activity distribution and image-derived input function and owing to the limited axial field-of-view of clinical PET scanners, full compartmental modelling can only be performed in the initial bed position. Dynamic imaging can reveal useful clinical information on normal and malignant tissues metabolic properties, e.g. the metabolic rate of glucose uptake. By the aid of micro- and macro-parametric metrics, tumor characterization and therapy response assessment will be facilitated. Despite the potential of parametric imaging in lesion detectability and reducing false-positive rate [3], this modality has been confined to research setting and single-bed FOVs.

A number of approaches were developed for the generation of parametric maps, such as Patlak method, spectral analysis and full compartmental modeling. Although graphical analysis is simpler, full compartmental modeling is more informative as it provides detailed physiological information on individual rate constants. The Generalized Linear Least Squares (GLLS) technique, as an algorithm for non-uniformly sampled biomedical systems, was adopted. In this work, we systematically compare lesion detectability between Patlak, GLLS and SUV ^{18}F-FDG WB clinical PET images for 8 patients focusing on interesting cases where full compartmental modeling provides additional information, mostly in the liver, not depicted by the other modalities.

II. Material and Methods

A. *Patient population and data acquisition*

The patient population included 8 adult patients (5 female and 3 males; mean age = 60.75±10.77years) referred for an ^{18}F-FDG PET/CT for staging or restaging. After injecting a standard dose of 3.5 MBq/kg (3.71±1.05MBq/kg) of ^{18}F-FDG; PET/CT scans were performed on a Siemens Biograph^{TM} mCT scanner. The scanning protocol lasted about 80 minutes and consisted of: (i) a low-dose CT for attenuation correction; (ii) a 6-min dynamic single-bed PET acquisition on the blood pool for extracting the input function (IF), starting simultaneously with ^{18}F-FDG injection; (iii) subsequently, 13 whole-body

N. Zaker is with the Division of Nuclear Medicine & Molecular Imaging, Geneva University Hospital, CH-1211, Geneva, Switzerland (e-mail: nedaza2011@gmail.com).

F. Kotasidis is with the Division of Nuclear Medicine & Molecular Imaging, Geneva University Hospital, CH-1211, Geneva, Switzerland (fkotasidis5@gmail.com).

V. Garibotto is with the Division of Nuclear Medicine & Molecular Imaging, Geneva University Hospital, CH-1211, Geneva, Switzerland (Valentina.Garibotto@hcuge.ch).

†H. Zaidi is with the Division of Nuclear Medicine and Molecular Imaging, Geneva University Hospital, CH-1211 Geneva, Switzerland, Geneva, Neuroscience Center, Geneva University, CH-1205 Geneva, Switzerland, and Department of Nuclear Medicine and Molecular Imaging, University of Groningen, University Medical Center Groningen, Groningen, Netherlands (e-mail: habib.zaidi@hcuge.ch).

978-1-7281-4164-0 /19/$31.00 ©2019 IEEE

PET scans, 3 min each, in continuous bed motion (CBM); (iv) and ~20 min SUV WB CBM scan acquired 60 min post-injection used as reference for comparison followed by (v) a contrast-enhanced CT scan (6/8 patients). 3D iterative OP-OSEM algorithm was used for image reconstruction using the clinical protocol with 2 iterations and 21 subsets including TOF and resolution modeling.

B. *Methodology for whole-body parametric imaging*

Patlak graphical analysis and GLLS are among the analysis methods used for image analysis. Multi-pass WB parametric imaging framework utilizes the Patlak method based on an irreversible two-tissue compartment kinetic model. Patlak analysis provides the influx constant rate (K_i) and distribution volume (V) macro-parameters representing the slope and the intercept of the standard Patlak model linear equation, respectively:

$$C(t) = K_i \int_0^t C_p(t)dt + VC_p(t) \quad (1)$$

The micro-parameters K_1 (plasma to non-phosphorylated compartment), k_2 (non-phosphorylated to plasma compartment), and k_3 (non-phosphorylated to plasma compartment) are the exchange rates between the 2 compartments of ^{18}F-FDG model. Although Patlak analysis is simpler and more robust, it can't use the potential of dynamic PET imaging to extract micro-parameters for improved lesion characterization. For full-compartmental modelling, there are different methods for parameter estimation. There is some evidence that the GLLS algorithm presents some advantages over other methods in non-uniformly sampled biomedical systems [4]. Among its benefits are (i) direct estimation of continuous model parameters; (ii) No requirement of initial parameter values; (iii) applicability to a variety of models with different structures; (iv) individual model parameters estimation as well as physiological parameters; (v) reasonable computational time requirement and (vi) production of unbiased estimates.

C. Image Analysis

SUV and contrast-enhanced CT images were evaluated qualitatively by an experienced physician producing a single report for each set of images summarizing the findings. Then macro- and micro-parametric images were produced using an in-house developed Matlab code. A head-to-head comparison of the different imaging modalities, including contrast-enhanced CT was performed. Malignant lesions (biopsy proven or previously known) which were just visible on contrast-enhanced CT images were also included. In cases where there is a noticeable number of lesions in a single organ or anatomical region, we assessed a maximum of 5 lesions to minimize the bias. 3D spherical VOIs were drawn manually on SUV and micro- and macro-parametric PET images of each lesion to estimate the relevant metrics at the same positions. If the lesions were non-metabolic and could not be seen on SUV images we used the CT-enhanced images for VOI delineation. In total, all SUV, macro- and micro-compartmental metrics were extracted from the same position. In addition, we defined additional VOIs on background regions far away from the lesions to calculate additional statistical parameters, such as the tumor to background ratio (TBR) and contrast to noise ratio (CNR), TBR and CNR scores were calculated using Eqs 2 and 3:

$$TBR = (\text{Tumour } ROI_{max}/\text{Background } ROI_{mean}) - 1 \quad (2)$$

$$CNR = TBR / \text{Background } ROI_{SD} \quad (3)$$

In addition, we used spearman's rank correlation coefficient (ρ) to assess the correlation between SUV_{max} and the maximum of the other metrics. A p-value less than 0.05 is considered as statistically significant.

III. Results and Discussion

In total, 104 lesions were detected in the 8 clinical studies among which 47 lesions were located in the bed position where the micro-compartmental parameters were available whereas the other 57 lesions were located outside this region. Hence, only Patlak macro-compartmental metrics and SUV were calculated for the later. Among these lesions, 16 were classified as known cancer and 5 as biopsy proven malignant lesions. Five clinical cases with discordant interpretation of the different modalities are discussed below. The first case consists of 3 lesions for one patient presenting with hepatocellular carcinoma (HCC) located in the liver. Two non-hypermetabolic liver lesions could be seen only on K_1 and k_2 images, whereas Patlak map was unable to detect it. Figure 1 shows one of these cases. This patient had also a treated liver lesion that could be seen as a cold spot in SUV, K_1 and blood volume images but K_i-Patlak was unable to detect it. The second interesting case is a liver lesion in a different patient categorized as recurrent HCC could be seen only in K_2 map (Fig. 2). Also we had a benign thyroid lesion that showed itself as hypermetabolic in SUV images but could not be seen on K_i-Patlak image and as hot spot in BV-Patlak image. Moreover, it can be seen in Table 1 that the correlation between SUV and K_i-GLLS is more significant comparing to the others.

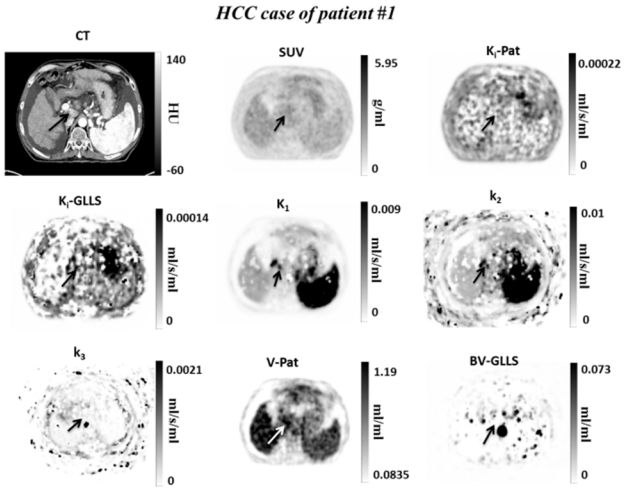

Figure 1. Hepatocellular carcinoma case (patient #1), non-hypermetabolic on SUV and K_i-Patlak images and detected on K_1 and k_2 images. Top panel (from left to right): Contrast-enhanced CT image, standardized uptake value (SUV) PET image, and Patlak-derived influx rate constant (K_i-Pat). Middle panel (from left to right): Generalized Linear Least Square (GLLS)-derived influx rate constant (K_i-GLLS), and rate constants (K_1 and k_2). Bottom panel (from left to right): Rate constant (k_3), Patlak-derived distribution volume (V-Pat) and GLLS-derived blood volume (BV-GLLS).

Table 1. Spearman's correlation (ρ) and p values (Sig.2-tailed) between suv and macro-parametric and micro-parametric images, calculated for the maximum values of lesions. Correlation is deemed significant for p<0.001. all values are reported for the full dataset and for the lesions grouped by localization.

	Suv & ki_pat	Suv & Ki_glls	Suv & K1	Suv & k2	Suv & k3
Total	0.761(p<0.001)	0.808(p<0.001)	0.481(p=0.001)	0.371(p=0.015)	0.395(p=0.01)
Abdominal	0.583(0.099)	0.9(p=0.037)	-0.1(p=0.873)	-0.1(p=0.873)	-0.3(p=0.624)
Liver	0.972(p<0.001)	0.853(p<0.001)	0.804(p=0.002)	0.573(p=0.051)	0.664(p=0.521)
Lungs	0.9(p=0.037)	0.8(p=0.2)	0.8(p=0.2)	0.8(p=0.2)	1(p<0.001)
Bones	0.945(p<0.001)	-	-	-	-
Lymph nodes	0.824(p<0.001)	0.846(p<0.001)	0.385(p=0.217)	0.147(p=0.649)	-0.077(p=0.812)
Other	0.251(p=0.348)	0.714(p=0.111)	0.486(p=0.329)	0.486(p=0.329)	0.086(p=0.872)

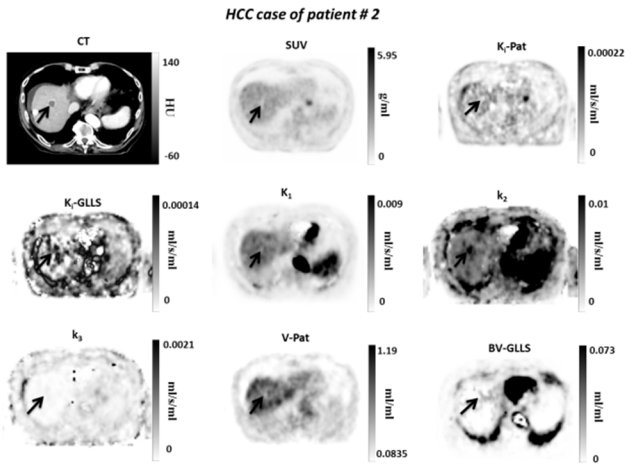

Figure 2. Case of a hepatocellular carcinoma (patient#2) detected only on k_2 image. The images shown are similar to Figure 1.

IV. CONCLUSION

This study demonstrated that multi-pass WB PET micro- and macro-parametric imaging may achieve equivalent or potentially superior lesion detectability and also less false-positives than standard-of-care SUV imaging with the advantage of producing all the set of images in only one session.

ACKNOWLEDGEMENTS

This work was supported by the Swiss National Science Foundation under grant SNSF 320030_176052.

REFERENCES

[1] N. Karakatsanis, M. A Lodge, A. Tahari, Y. Zhou, R. Wahl, and A. Rahmim, *Dynamic whole-body PET parametric imaging: I. Concept, acquisition protocol optimization and clinical application Phys Med Biol*. 2013;58:7391-7418.

[2] A. F. Kotasidis, V. Garibotto, and H. Zaidi, "Patient-Specific Hybrid Whole-body PET Parametric Imaging From SpeedModulated Continuous Bed Motion Dynamic Data," in *2017 IEEE Nuclear Science Symposium and Medical Imaging Conference (NSS/MIC)*, 2017, pp. 1-2.

[3] G. Fahrni, N. A. Karakatsanis, G. Di Domenicantonio, V. Garibotto, and H. Zaidi, "Does whole-body Patlak 18 F-FDG PET imaging improve lesion detectability in clinical oncology?," *Eur Radiol*. 2019;29:4812-4821.

[4] W. Cai, D. Feng, R. Fulton, and W.-C. Siu, "Generalized linear least squares algorithms for modeling glucose metabolism in the human brain with corrections for vascular effects," *Comput Methods Programs Biomed,* vol. 68, pp. 1-14, 2002.